Experimental Investigation of Flexural Behaviour of Conventionally Reinforced Concrete Beams Strengthened with Near-surface-mounted Mild Steel Strips

N. J. Ateny[1*], David O. Koteng[1,2], S. M. Shitote[1,3]

[1]Department of Civil Engineering, Pan African University Institute for Basic Sciences, Technology and Innovation, Juja, Kenya.
[2]Department of Civil and Resource Engineering, Technical University of Kenya, Nairobi, Kenya.
[3]Department of Civil and Structural Engineering, Moi University, Eldoret, Kenya.

ABSTRACT: Due to material degradation with age, design and construction inaccuracies, reinforced concrete (RC) beams may develop flexural strength deficiencies during service life and require strengthening. This study experimentally investigates the flexural performance of RC beams strengthened with near-surface-mounted (NSM) hot-rolled mild steel strips, considering the influence of pre-loading conditions on the effectiveness of the strengthening. Flexure-dominant beams were tested under four-point loading, and performance was evaluated in terms of peak load capacity, elastic stiffness, and energy absorption derived from load–deflection responses. Results showed that NSM strengthening increased flexural capacity by 30% and 53% for preloaded and directly strengthened specimens, respectively, compared to the control beam, although failure in strengthened beams was governed by shear rather than flexure, indicating a shift in the critical failure mode following strengthening. Elastic stiffness improved by 3% and 49% for preloaded and directly strengthened specimens, respectively, while energy absorption decreased by 65% and 63%, reflecting reduced ductility and a shift toward more brittle behaviour. Notably, NSM strengthening altered the governing failure mode from ductile flexural failure in the control beam to brittle shear failure in the strengthened beams, a significant behavioural shift with important design implications. A design equation to estimate the required area of steel strips for retrofitting was derived from EC2-based sectional analysis and modified to account for near-surface strips.

KEYWORDS: conventional reinforcement, flexural strengthening, mild steel strips, retrofitting, moment capacity, near-surface mounted technique

[Received May. 16, 2026; Revised Jun. 04, 2026; Accepted Jun. 17, 2026] Print ISSN: 0189-9546 | Online ISSN: 2437-2110

I. INTRODUCTION

Reinforced concrete (RC) structures gradually lose strength with age due to deterioration of reinforcement or degradation of concrete cover (Hashemi, 2011). Deficiencies may also arise from increased service loads, construction inaccuracies, or detailing errors, as noted in Askar, Hassan and Al-Kamaki (2022), making strengthening necessary to restore flexural or shear capacity. Common retrofitting methods include externally bonded reinforcement (EBR) or near-surface-mounted (NSM) techniques using steel, FRP, or concrete jacketing (Rasheed *et al.*, 2010; Aykac *et al.*, 2012; Oller, Pujol and Marí, 2019; Raza *et al.*, 2019; Awad, Husain and Fawzy, 2022; Hamoda *et al.*, 2024; Hosen *et al.*, 2024). The NSM method is often preferred over EBR due to reduced risk of debonding and better protection from environmental exposure (Hanu and Subha, 2018). Numerous studies have investigated strengthening methods to better understand the behaviour and failure mechanisms of retrofitted beams and to develop more efficient rehabilitation approaches.

Zhang, Yu and Chen (2017) examined the behaviour of RC beams strengthened with NSM carbon fibre reinforced polymer (CFRP) strips compared with CFRP rods. The study reports improved bond performance in strip-strengthened beams due to the higher perimeter-to-cross-sectional area ratio of strips. A similar study by Sabau et al. (2018) investigated side-mounted (S-NSM) and bottom-mounted (B-NSM) reinforcement for flexural strengthening. The S-NSM configuration improved resistance to early concrete cover debonding, increased crack distribution, and enhanced energy absorption, whereas B-NSM beams achieved higher flexural capacity owing to a larger lever arm. Other investigations such as the Rizzo and De Lorenzis (2009) study show that NSM technique achieves more significant strength improvement compared to the EBR technique. Shear-deficient RC beams, strengthened with U-shaped FRP through the EBR technique and NSM FRP strips, were tested in the study. The findings indicate a shear capacity increase of up to 44% for NSM strengthening compared with 16% for EBR applications, highlighting the effectiveness of the NSM approach.

Despite extensive research on FRP-based strengthening, comparatively fewer studies have explored the use of mild steel as a strengthening material. Although mild steel possesses lower tensile strength than FRPs, its high ductility provides significant deformation capacity, allowing for more

*Corresponding author: bjohnateny@gmail.com

doi: http://doi.org/10.63746/njtd.v23i2.4797

gradual failure and improved warning prior to collapse (Farooq *et al.*, 2026).

Recent investigations involving steel strips for strengthening of RC structures have primarily focused on prestressed steel and/or high yield steel applications. Moghaddam et al. (2010) experimentally examined concrete columns retrofitted with prestressed steel strips and demonstrated effective active confinement that reduced crack development. Similarly, Tarabia and Albakry (2014) considered high yield steel strips and angles, studying their strengthening effect on structural behaviour of RC columns; and showed that the steel strips and angles significantly enhanced columns capacity under axial loads. These studies were, however, limited to column behaviour, leaving the applicability of similar techniques to beams insufficiently explored. Yang et al. (2022) proposed a steel-strapping method derived from the packaging industry for enhancing beam shear capacity, reporting increases of 95% in shear strength and 88% in displacement capacity. In addition to using a different steel type, the study focused solely on shear behaviour and did not consider the effect of strips in enhancing flexural capacity; while employing the EBR technique, which may present durability concerns due to external exposure of the strengthening material. Furthermore, the steel-strapping method can be technically demanding to apply and may present accessibility challenges, particularly in developing regions. A similar study by Hamoda et al. (2022) experimentally tested beams, strengthened with ECC and stainless-steel strips, for flexural strength; reporting a 156% improvement in flexural capacity of the beams. Despite the significant effectiveness of the proposed strengthening in the study, its more hybrid nature introduces additional costs that make it relatively more expensive than simply using mild steel bonded with structural epoxy. Most of the other studies incorporating steel strips for structural strengthening are largely focused on investigations of structural behaviour of either RC or masonry walls, and do not isolate the applicability to beams (Altin, Kopraman and Baran, 2013; Farooq, Shahid and Ilyas, 2014; Jing, Krevaikas and Zhang, 2021).

The present study addresses these gaps by investigating the flexural performance of RC beams strengthened with NSM hot-rolled mild steel strips — an accessible, ductile, and cost-effective alternative to FRP systems, high yield and prestressed steel— while additionally examining the influence of preloading condition on strengthening effectiveness. Unlike FRP materials, mild steel is widely available and inexpensive, requiring no specialist handling or equipment. This makes it a particularly attractive option in developing regions where FRP systems may be costly or difficult to source. A rational design expression specifically for NSM mild steel strip flexural strengthening of beams has not been established in the reviewed literature. This study addresses this by deriving a design equation from EC2 sectional analysis principles, modified to incorporate the contribution of NSM mild steel strips as additional tensile reinforcement. The objective of this study is therefore to experimentally investigate the flexural performance of RC beams strengthened with NSM hot-rolled mild steel strips, and to evaluate the influence of preloading condition on strengthening effectiveness in terms of load capacity, elastic stiffness, and energy absorption.

II. THEORETICAL ANALYSIS

The analytical framework of this study is grounded in Euler–Bernoulli beam theory, which postulates that cross-sections of a beam remain plane and perpendicular to the neutral axis during bending. This establishes a linear strain distribution across the beam depth, providing the strain compatibility conditions necessary to relate the deformations of concrete, conventional reinforcement, and the near-surface mounted steel strips consistently. Sectional analysis theory, as codified in Eurocode 2, builds on this by invoking force and moment equilibrium principles to predict the moment capacity of the strengthened sections. The compressive behaviour of concrete is described using the equivalent rectangular stress block theory, a widely accepted idealization that simplifies the nonlinear stress distribution in the compression zone into a uniform stress acting over an effective depth, rendering the equilibrium equations analytically tractable without significant loss of accuracy.

The contribution of the NSM mild steel strips is treated theoretically as that of additional tensile reinforcement, consistent with the assumptions of classical reinforced concrete theory, with both the conventional rebars and the strips assumed to develop their full yield strength at the ultimate limit state. Performance evaluation of the beams further draws on energy methods in structural mechanics, whereby energy absorption is interpreted as the total internal strain energy stored during loading and elastic stiffness as the resistance of the beam to initial elastic deformation — both derived from the load–deflection response of the tested specimens.

III. MATERIALS AND METHODS

A. Material characteristics, mix design and specimen construction

Aggregates with properties shown in Table 1 were used for normal concrete (NC). The physical and mechanical properties of the aggregates were determined to aggregate materials testing code, EN 1097-2 (1998), and comply with the standard requirements of aggregates compliance code, EN-12620, (European Committee for Standardization, 2002). Portland pozzolana CEM II/B-R 42.5 cement was used. This cement is manufactured in Kenya to Kenyan standard, KS EAS 18-1 (2018), that conforms to requirements of cement compliance code, EN 197-1, (European Committee for Standardization, 2000).

Table 1 Properties of aggregates

Type of Aggregate	Fineness Modulus	Specific gravity	Water absorption	Aggregate crushing value	Aggregate impact value
Fine aggregate	4.03	3.1	2.4%	-	-
Coarse aggregate	-	2.6	3.3%	13.25%	5.46%

Mix proportions of the NC, designed to the method of the British Department of the Environment (Marsh, 1997), are shown in Table 2. Cubes and cylinders were cast and tested after 7, 14 and 28 days for compressive cube/cylinder strength and tensile split strength as shown in Fig. 1a-b respectively. Specimen preparation and testing were done according to the hardened concrete testing codes, BS EN12390-1-6 (2002). Table 3 shows the mechanical properties of the NC from the respective tests at 7, 14 and 28 days.

Table 2 Mix proportions of normal concrete

Cement (kg/m3)	Fine Aggregate (kg/m3)	Coarse Aggregate (kg/m3)	Water (kg/m3)
472	701	857	250

Table 3 Mechanical properties of concrete

Age (days)	Compressive cube strength (MPa)	Compressive cylinder strength (MPa)	Tensile split strength (MPa)
7	26.30	19.04	2.46
14	33.41	24.73	2.85
28	36.72	29.38	3.14

A characteristic cylinder strength of 25 MPa was used for NC mix design, and it can be seen from Table 3 that the characteristic cylinder strength of the concrete, made from the mix shown in Table 2, at 28 days is greater than 25 MPa, hence, acceptable.

The mechanical properties of Sikadur®-31 CF Slow structural epoxy, as provided in the manufacturer's product data sheet, are shown in Table 4. Properties are reported for a 1-day curing period at +25°C, consistent with the curing duration adopted in this study.

Table 4 Mechanical Properties of structural epoxy

Property	Value (N/mm²)	Test Standard
Compressive Strength	30	DIN EN 196
Tensile Strength in Flexure	20	DIN EN 196
Tensile Strength	6	DIN EN 196

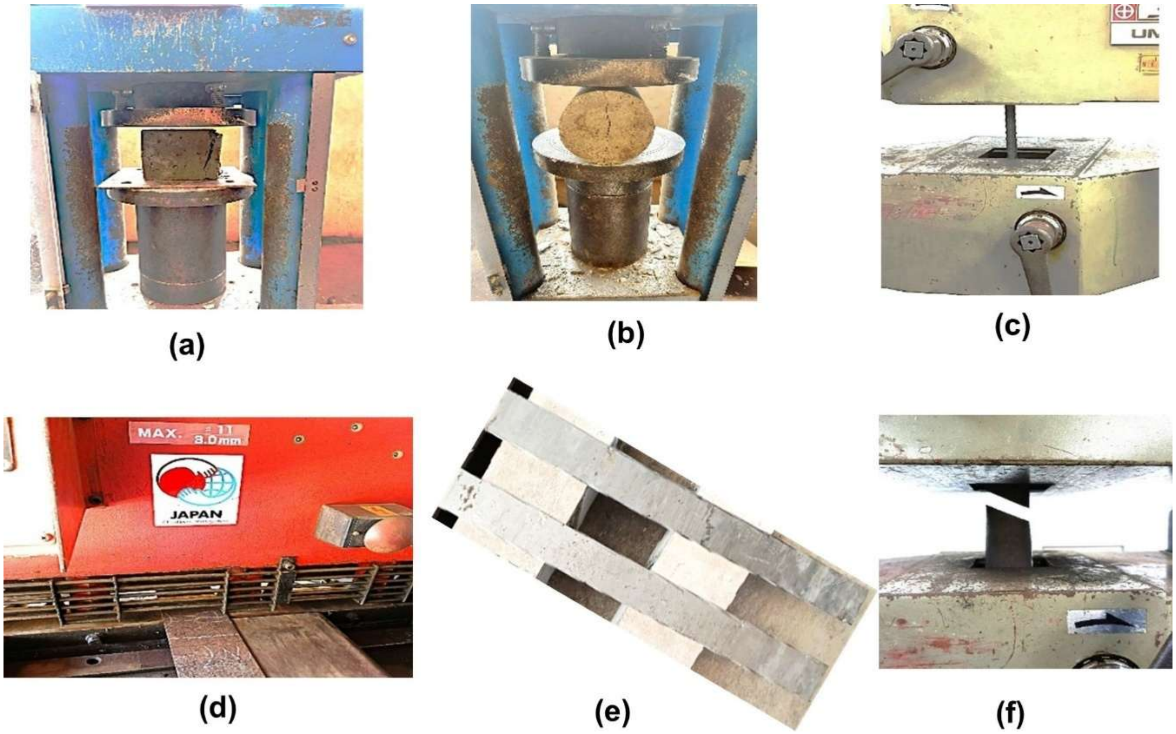

Fig. 1 Materials tests: (a) Compressive cube strength, (b) Splitting tensile strength, (c) Tensile test of rebar and (d) - (f) Preparation and testing of steel strips

High yield ribbed tensile rebars of diameters 8 mm, 10 mm and 12 mm, were used as conventional reinforcements in the beams. Mild steel strips with dimensions as detailed in Fig. 3, were obtained by carefully cutting off from a 2400 mm x 1200 mm x 2.2 mm hot rolled mild steel plate using a guillotine shearing machine as shown in Fig. 1d-e. Specimens of rebars and mild steel were both prepared and tested for mechanical properties to metallic material testing code, EN ISO 6892-2 (2019), as shown in Fig. 1c and 1f. The mechanical properties of steel rebars and strips are shown in Table 5. The elastic modulus is taken as the nominal value for steel.

Table 5. Mechanical properties of steel

Property	Reinforcing bars			Steel strip
Diameter/thickness (mm)	8	10	12	2.2
Yield strength (N/mm²)	651.21	643.62	465.90	211.61
Tensile strength (N/mm²)	744.38	728.93	606.41	317.57
Elastic modulus (N/mm²)	205000	205000	205000	205000
Elongation (%)	4.75	7.52	13.78	11.24

B. Details of tested specimens

A total of nine 1000 mm x 250 mm x 200 mm beam specimens were tested. The beams were reinforced with two 12 mm diameter tensile rebars; two 10 mm diameter rebars in the compression zone; and 8 mm diameter stirrups at 100 mm spacing as shown in Fig. 2, giving tensile and compression reinforcement ratios of 0.43% and 0.30% respectively. These reinforcements were designed to Eurocode 2 (EC2), European Committee for Standardization (2004), so that the approximate theoretical load capacity of the beams would be at least 15% of maximum capacity of the laboratory testing frame. The shear reinforcement was designed and detailed in accordance with EC2, with the 100 mm stirrup spacing deliberately provided closer than the code minimum to keep the beams flexure-dominant. In this regard, the theoretical flexural capacity of the control beam, calculated using EC2 sectional analysis, with unfactored material strengths, was 22.53 kNm, corresponding to a theoretical load capacity of approximately 150.2 kN under the four-point loading arrangement in Figure 5a. The theoretical shear capacity, calculated considering 8 mm stirrups at 100 mm spacing, was 236.6 kN — approximately 60% greater than the flexural load capacity, confirming the intended flexure-dominant failure sequence prior to testing.

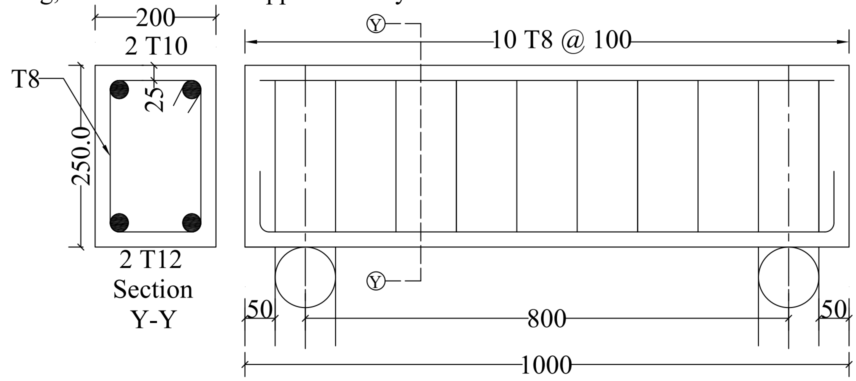

Fig. 2. Conventional reinforcement details.

The main parameter of interest was the preloading condition, and beams were categorized into preloaded beams, B-Pld, and directly strengthened beams, B-Str as shown in Table 6. Preloading in the B-Pld beams was done to simulate existing weakness in normal concrete beams, and was done by initially loading to approximately 42% of the ultimate load of the control beam. B-Str beams simply had no weakness initially induced in them, and were thus directly strengthened. The B-Str beams were strengthened with two longitudinal tensile steel strips with dimensions measuring 950 mm × 50 mm × 2.2 mm as shown in Fig. 3, while the already weak B-Pld beams were retrofitted similarly. The strip length was determined by the available bonding length after accounting for concrete cover at both ends. The strip width was selected such that the combined cross-sectional area of the two strips was approximately equal to that of the two 12 mm diameter tensile rebars. The strip thickness of 2.2 mm was chosen consistent with the findings of Aykac et al. (2012), which recommend thinner steel plates within the range of 1.5–6 mm to improve composite action with the surrounding concrete. Control specimens, B0, were constructed to act as benchmarks for comparison.

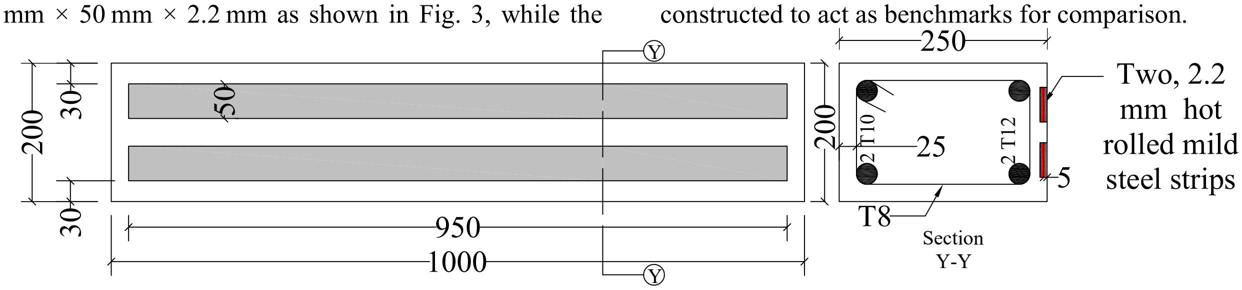

Fig. 3 Mild steel strips details

Table 6 Tested specimens

Specimen Name	Preloading condition
B0	N/A
B-Pld	Weakened to 42% of B0 ultimate load
B-Str	As-intact

The nine beam specimens were prepared to details shown in Fig. 2. FLAB-6-11-3LJC-F strain gauges were attached to mid points of tensile steel for strain monitoring at critical tensile locations, Fig. 4a. Strain instrumentation was concentrated at the midspan tensile reinforcement, consistent with the flexure-dominant design intent of the specimens; shear-span instrumentation was therefore outside the planned experimental scope. All specimens were then cast with the NC made using a concrete mixer as shown in Fig. 4b, following the mix design in Table 2, and cured for 28 days under room temperature.

Grooves of 950 mm x 55 mm x 12.2 mm were then created on the beams, using a concrete cutter machine to carefully cut off the 12.2 mm concrete cover, as shown in Fig. 4c. The groove depth of 12.2 mm corresponded to the concrete cover thickness, minimizing section loss while providing adequate embedment for the strips. The groove width of 55 mm accommodated the 50 mm strip width with a 2.5 mm clearance on each side for epoxy application. No grooves were created on the control specimens in each beam group. Prior to bonding, the steel strip surfaces were cleaned to remove dust, grease, and loose particles, consistent with the manufacturer's surface preparation requirements for steel substrates. Sikadur®-31 CF Slow structural epoxy was then applied to the cut concrete surfaces, and mild steel strips bonded to concrete by means of the epoxy, Fig. 4d. Concrete was then applied to re-cover the strips as shown in Fig. 4e. The reinstated concrete cover restored the original section geometry and provided full encasement of the strips, contributing to composite action and durability. The epoxy adhesive was applied according to the product application specification for sufficient bond. The beams were left for 24 hours to allow for adequate curing of the structural epoxy and then tested the following day.

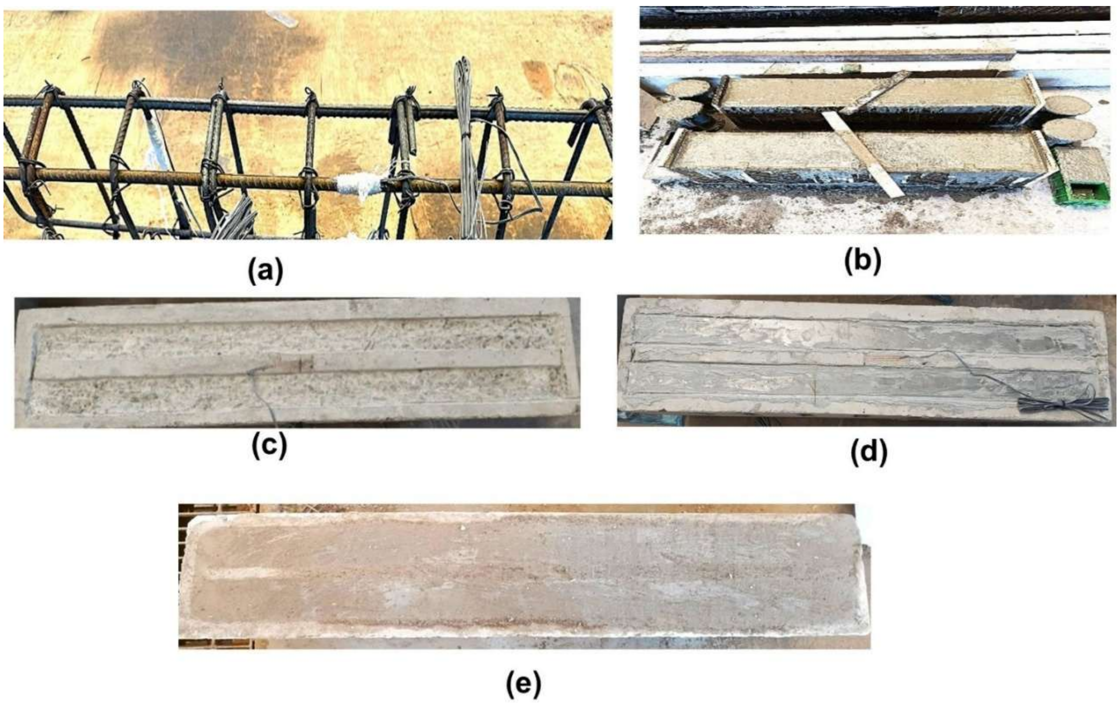

Fig. 4 Specimen construction: (a) Reinforcement cage, (b) Beams casting, (c) Grooves cutting, (d) Bonding of strips and (e) Applying concrete cover

C. Experimental set up and instrumentation

The beams were tested under four-point loading as shown in Fig. 5a-b. Concrete strain gauges were installed at mid spans of tensile and compressive faces of the beams. The set up consisted of beams resting on two roller supports with centres 100 mm from each end of the beam. A Linear Variable Differential Transformer (LVDT) was installed right below the midpoint in the tensile face, to measure deflections at midspan. Loading, measured with a load cell, was then applied by means of a hydraulic jack through a loading plate that transferred the load to the beam through rollers. The data acquisition system consisted of a data logger to which the strain gauges, LVDT and the load cell were connected. The actual laboratory set up is as shown in Fig. 5b. All beams were tested to failure with incremental loading of approximately 5 kN, selected based on the capacity and sensitivity of the load cell. With a 500 kN capacity load cell, the 5 kN increment represents 1% of full scale, well within the reliable measurement range of the instrumentation.

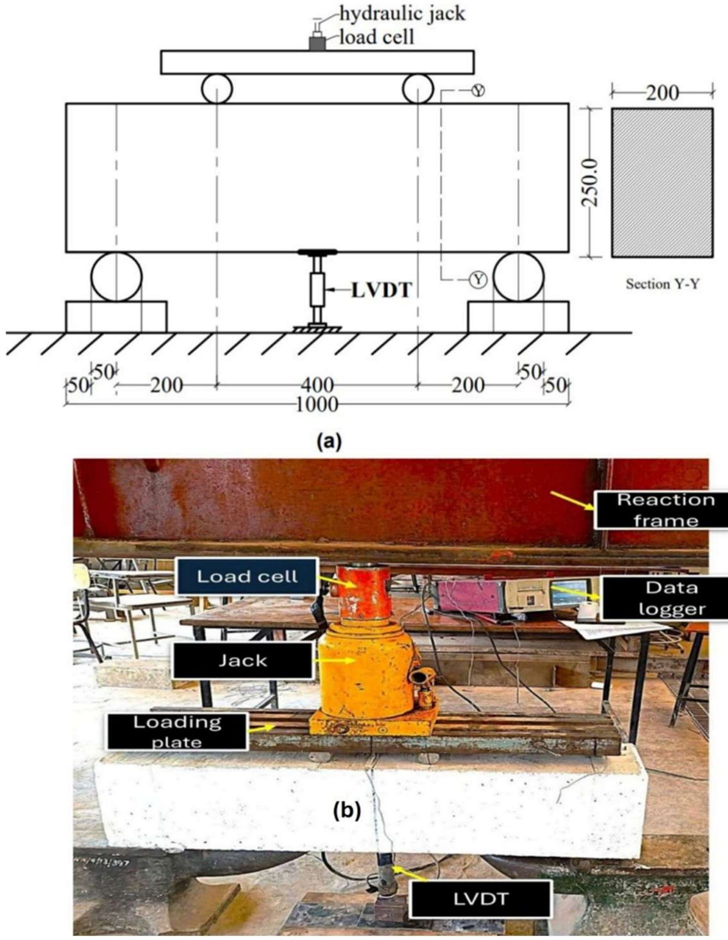

Fig. 5. Test set up: (a) Schematic of set up and (b) Actual laboratory set up.

IV. Results and Discussion

Three specimens were tested per configuration to ensure repeatability. For each configuration, the individual load-deflection data from the three replicas were averaged to produce a single representative load-deflection curve, from which all reported parameters were derived.

Table 7 shows results of the tested beams. They include values of loads and deflections at first crack and failure respectively (Pcr, Pu and Δ_{cr}, Δ_u); peak energy absorption and elastic stiffness. The failure modes of the respective beams are also noted. These parameters are discussed in detail in the subsequent sections.

Table 7 Flexural test results

Specimen label	Cracking stage		Peaked stage		Energy absorption, E and elasticity stiffness, K		
	P_{cr} (kN)	Δ_{cr} (mm)	P_u (kN)	Δ_u (mm)	E (kNmm)	K (kN/mm)	Failure mode*
B0	76	0.43	180	20.50	3122	50.96	F+C
B-Pld	151	1.72	235	6.18	1102	52.283	S
B-Str	174	1.42	276	7.32	1156.25	76.11	S

* S: shear failure; C: concrete crushing; F: flexural failure

*Corresponding author: bjohnateny@gmail.com
doi: http://doi.org/10.63746/njtd.v23i2.4797

(a) (b) (c)

Fig. 6 Failure modes and crack patterns. (a) Control specimen, (b) B-Pld and (c) B-Str.

A. Modes of failure and crack patterns

Fig. 6 shows the failure modes and crack patterns of the tested beams. The control specimen first developed flexural cracks at the tension face, which progressively widened and propagated vertically with increasing load, followed by crushing of concrete in the compression zone, Fig. 6a, indicating typical flexural failure. In strengthened specimens B-Pld and B-Str, initial flexural cracks appeared at higher loads compared to the control beam, demonstrating delayed cracking and increased stiffness due to the NSM mild steel strips. These cracks remained limited in propagation, after which diagonal cracks developed within the shear span and widened progressively along the line between the loading point and support, leading to shear splitting failure, Fig. 6b–c. The considerably larger increase in cracking load relative to ultimate capacity is attributable to the NSM strips' influence on pre-cracking behavior. Being fully encased in concrete following cover replacement, the strips stiffened the tension zone and resisted tensile stresses alongside the concrete, pushing the cracking load significantly higher. Once cracking initiated, shear failure governed before the strips could be fully mobilized, which moderated the gain in ultimate capacity relative to the gain in cracking load.

The strengthening increased flexural resistance and altered the internal stress distribution, redistributing forces toward the shear spans. Consequently, failure shifted from flexure to shear, indicating that shear resistance governed the ultimate behavior of the strengthened beams. By enhancing the flexural resistance of the midspan section, the NSM strips effectively redistributed internal forces toward the shear spans, reducing the shear reserve relative to the increased flexural capacity. Although the beams were originally designed with a 60% shear capacity excess over flexural capacity, this reserve proved insufficient following strengthening. The shear failure was largely attributed to excessive flexural strengthening, as the steel strips were initially selected based on the equivalent area of conventional tensile reinforcement, which introduced over-reinforcement and consequently triggered premature shear failure. This highlights the need for a rational design approach when selecting the area of retrofitting steel strips. Specifically, the required strip area should be determined with reference to the target bending moment capacity of the section, rather than the area of existing conventional reinforcement, as proposed in the design equation derived in this study. Additionally, to mitigate the risk of shear failure following flexural strengthening, the provision of supplementary shear reinforcement — such as transverse steel strips — is recommended, particularly in beams where shear capacity is not significantly in excess of flexural capacity.

B. Peak loads

From Table 7, it can be seen that the beams resisted loads to ultimate values of 180 kN, 235 kN and 276 kN as B0, B-Pld and B-Str respectively. It is clear from this observation that loads at peak for beams initially weakened in flexure, and those directly strengthened are higher than that of the control at peak by about 30% and 53% respectively. This demonstrates the contribution of mild steel strips in enhancing the moment capacities of the treated specimens, which then allowed these beams to resist more load at failure. Mounting steel strips in an attempt to alleviate the effect of weakening, simulated by preloading, achieves a 30% improvement in flexural strength which is significantly less than the effect achieved when the beam is strengthened prior. Nevertheless, the findings still show that mild steel strips can be used as a successful retrofitting or strengthening option for beams deficient in flexural strength.

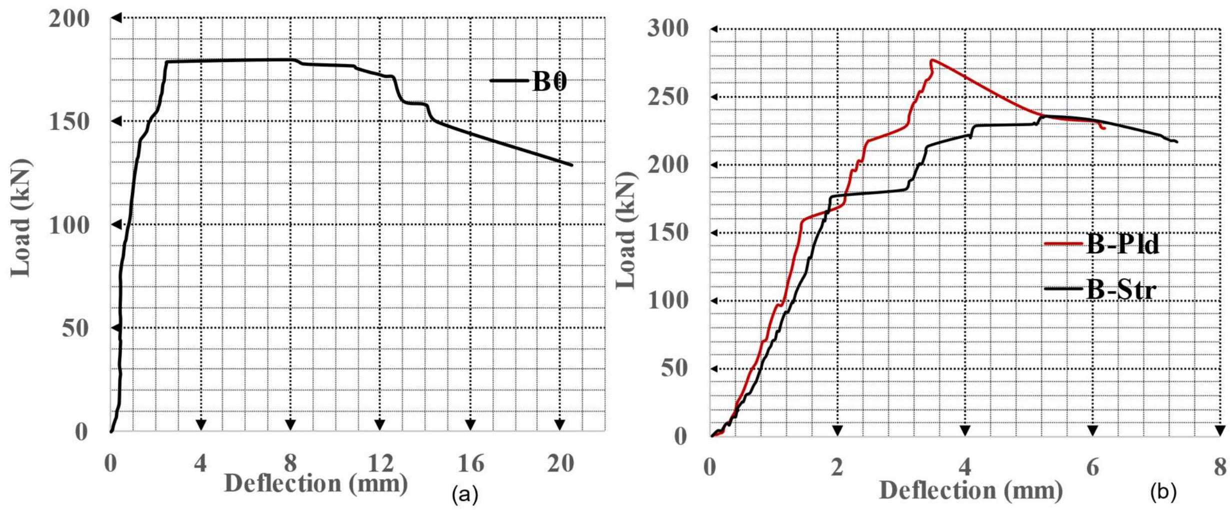

Fig. 7 Load-deflection relations of tested specimens

C. Load deflection relationships

The load–deflection curves for all tested specimens are as shown in Fig. 7. The control specimen (B0) exhibited typical flexure-dominant behavior, Fig. 7a, with a nearly linear load–deflection response up to the first crack at 76 kN, reaching a peak load of 180 kN and a maximum deflection of approximately 20.5 mm before failing in flexure. In comparison, the treated specimens—both preloaded and directly strengthened beams—showed higher elastic stiffness and reduced softening, Fig. 7b. Their curves rose steeply to first crack loads of approximately 151 kN and 174 kN, respectively, with minor curvature changes beyond these points, indicating limited stiffness reduction at cracking. The loads then reached peak values with minimal post-peak decrease, reflecting a brittle failure dominated by shear, which is attributed to the flexural strengthening effect of the NSM mild steel strips.

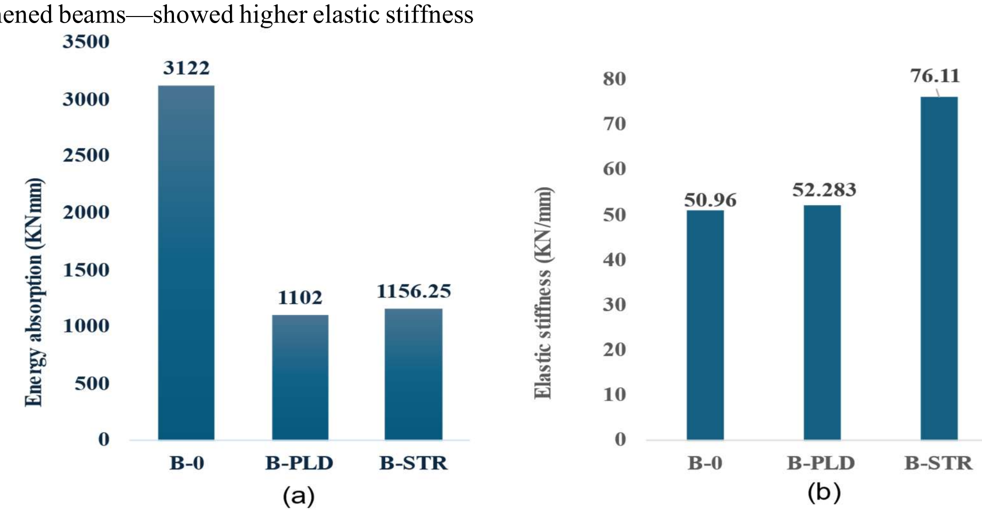

Fig. 8. Energy absorption and elastic stiffness of tested specimens

D. Elastic stiffness and energy absorption

The values of elastic stiffness and energy absorption for the tested specimens are shown in Table 7. Fig. 8 shows the comparisons of energy absorption and elastic stiffness for all the beams. Energy absorption, E, was considered as the total energy that developed internally during loading to failure. This was numerically determined using the trapezoidal rule, whereby the area under the load-deflection curve was computed as the sum of trapezoidal areas between consecutive data points. The elastic stiffness, K was assumed as the value of the slope for the first linear portion of the load-deflection curve for all the beams. Table 7 shows that elastic stiffness is generally higher in B-Pld and B-Str beams as compared to the control, B0. It can be seen that only the directly strengthened beams show a considerable increase in the K value compared to the control with about 49% increase. The preloaded beam however attained an elastic stiffness just 3% higher than the control, an inconsistency which can be explained by the effect of weakening caused by preloading.

Energy absorption, however, showed an opposite trend, with the control beam demonstrating substantially higher energy absorption, exceeding the preloaded and directly

*Corresponding author: bjohnateny@gmail.com
doi: http://doi.org/10.63746/njtd.v23i2.4797

strengthened specimens by about 65% and 63%, respectively. Energy absorption is governed by both the magnitude of load resisted and the deformation capacity of the beam. In the control beam, ductile flexural failure allowed for significant post-peak deformation, producing a broad load-deflection response and consequently high energy absorption. In the strengthened beams, however, failure shifted from ductile flexure to brittle shear, fundamentally altering the shape of the load-deflection curve. The steeper initial slope due to enhanced stiffness, combined with abrupt loss of load capacity at shear failure and minimal post-peak deformation, produced a much narrower area under the curve. Increased stiffness also reduced crack propagation and widening, further limiting deformation capacity. Despite higher load resistance, energy absorption was therefore lower in the strengthened beams. The results indicate that energy absorption is not simply a function of strength — it is critically dependent on the prevailing failure mechanism and the associated deformation behavior.

From a serviceability perspective, the NSM strips offered notable practical benefits. The higher elastic stiffness in the strengthened beams indicates better resistance to deformation under service loads — relevant to deflection control at the serviceability limit state. Crack initiation was also delayed considerably, occurring at 99% and 129% above the control cracking load for B-Pld and B-Str respectively. This has direct implications for durability, as delayed cracking reduces the exposure of internal reinforcement to potentially aggressive environments.

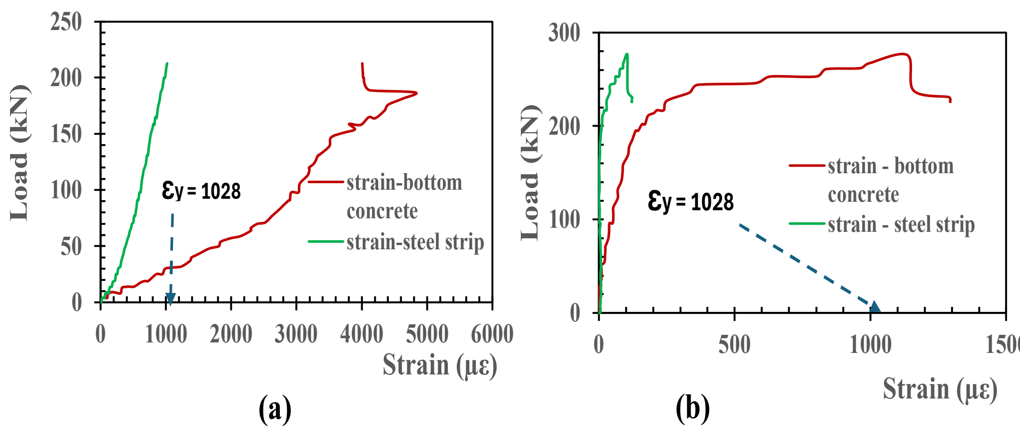

Fig. 9 Load-strain responses of tested specimens: (a) B-Pld and (b) B-Str.

E. Strain analysis in the strips

The load–strain relationships for the preloaded and directly strengthened specimens are presented in Fig. 9. Strain was measured at the concrete bottom fibre to provide an indication of crack initiation and progression. As shown in Fig. 9a, the preloaded beam exhibited a gradual increase in steel strip strain from the onset of loading to failure, corresponding with the development and widening of concrete cracks, indicating effective crack restraint provided by the strengthening strips. Stress redistribution occurred immediately upon reloading, with tensile forces shared between the conventional reinforcement and the external steel strips. This behavior is attributed to prior preloading of the beam up to 42% of control beam ultimate load, which reduced the tensile contribution of concrete during subsequent loading after strengthening. The steel strips did not reach yielding (maximum strip strain is less than the theoretical yield strain, ε_y = 1028με), as failure shifted to a shear-dominated mode due to the enhanced flexural capacity resulting from strengthening. In contrast, Fig. 9b shows that the directly strengthened specimen exhibited negligible strip strain at loading onset, with strip activation occurring only after crack initiation, identified by a sudden change in the slope of the concrete strain curve. Following cracking, strip strain increased approximately linearly with applied load, indicating immediate redistribution of tensile forces into both the strengthening steel strips and the conventional reinforcement. Similar to the preloaded specimen, yielding of the steel strips was not achieved because failure was governed by shear rather than flexure. Overall, the observed strain responses indicate that activation of the strengthening steel strips is governed by crack formation and load-path redistribution, with the enhanced flexural capacity shifting the governing failure mode from flexure to shear before yielding of the strips could be achieved. The fact that the strips did not yield has an important implication — it means the full tensile capacity of the strengthening system was not mobilized during testing. The observed capacity improvements of 30% and 53% therefore reflect only a partial contribution of the NSM mild steel strips, and higher gains would likely be achieved if flexural failure were allowed to govern. This reinforces the need for rational strip area selection, as addressed by the proposed design equation, to avoid the over-reinforcement that caused premature shear failure in this study. No debonding indicators, including audible cracking, visible strip separation, or epoxy interface failure, were observed in any specimen throughout testing, confirming adequate bond performance of the NSM system.

V. Determination of required area of steel strips: design equation

The amount of retrofitting mild steel strips used during experimentation was initially selected based on the equivalent area of the conventional tensile reinforcement provided in the control beams. Experimental results indicated, however, that this approach resulted in excessive flexural strengthening, leading to premature shear failure instead of the desired flexural mode of failure. A rational design expression is therefore required to estimate the necessary area of steel strips corresponding to a target bending moment.

Moment capacity was derived using sectional analysis, Fig. 10a-c, based on EC2 section analysis principles, European Committee for Standardization (2004), modified to incorporate the contribution of near-surface mounted steel strips acting as additional tensile reinforcement. Plane sections were assumed to remain plane in accordance with the Euler–Bernoulli beam theory (Haukaas, 2026). The equivalent rectangular stress block, which approximates the idealized parabolic–rectangular stress–strain relationship for concrete, was employed. Both the internal tensile reinforcement and the NSM mild steel strips were assumed to reach their design yield strength at the ultimate limit state. Strip yielding was not observed in the current experiments due to premature shear failure. However, the assumption remains valid as a design basis, since the equation is intended to guide strip area selection toward a target moment capacity under flexure-governed conditions, where yielding of both steel systems would be expected.

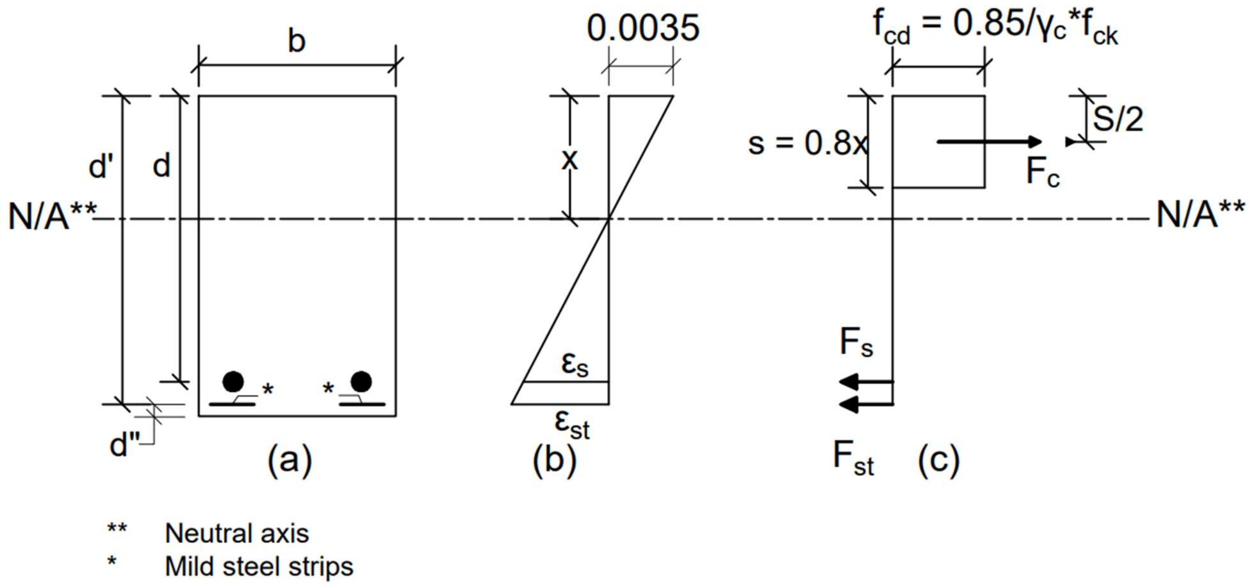

Fig. 10. Sectional analysis of strengthened beams: (a) Beam cross section, (b) Strain profile and (c) Stress distribution.

A. Moment capacity, M_{Rd}

Force equilibrium requires that,

$$F_c = F_{st} + F_s \tag{1}$$

$$0.8xbf_{cd} = A_s f_{yd} + A_{st} f'_{yd} \tag{2}$$

Where F_c is resultant compressive force of the rectangular stress distribution in concrete; F_{st} and F_s are tensile forces in steel strip and conventional steel reinforcements respectively; f_{cd}, f_{yd} and f'_{yd}, are the design compressive strength of concrete, design yield strength of conventional reinforcement and design yield strength of mild steel strips respectively; A_s and A_{st} are areas of conventional steel and mild steel strips respectively. x is depth to the neutral axis.

Moment equilibrium at the compression face requires that,

$$M_{Rd} = A_s f_{yd} d + A_{st} f'_{yd} d' - 0.8xbf_{cd} \times 0.4x \tag{3}$$

Where d and d' are the effective depth to centers of conventional tension steel and mild steel strips respectively; and $d' = h - d"$; h being the overall depth of the section and $d"$, the distance to center of strip from groove cover.

Expressing the neutral axis depth in Eq. (3) in terms of design strengths of concrete, conventional steel and mild steel strip; b and the respective areas of the steel rebars and strips; and setting $\alpha_1 = \frac{f_{yd}}{f_{cd}}$; and $\alpha_2 = \frac{f'_{yd}}{f_{cd}}$, the moment capacity of the section can be determined from Eq. (4).

$$M_{Rd} = \alpha_1 f_{cd} d A_s - \frac{\alpha_1^2 f_{cd}}{2b} A_s^2 + \left(\alpha_2 d' - \frac{\alpha_1 \alpha_2 A_s}{b}\right) f_{cd} A_{st} - \frac{\alpha_2^2 f_{cd}}{2b} A_{st}^2 \tag{4}$$

The limiting value of the moment capacity of the section should be the same as the ultimate bending moment in the beam, M, i.e., $M_{Rd} \geq M$.

B. Area of required mild steel strips for retrofitting

The area of the required steel strips for strengthening can then be determined from Eq. (7), which is the solution of the quadratic Eq. (6). The quadratic equation is obtained by establishing constants q_1, q_2 and q_3, shown in Eq. (5), from Eq. (4), noting $M = M_{Rd}$.

$$q_1 = \frac{\alpha_2^2 f_{cd}}{2b};\ q_2 = -\left(\alpha_2 d' - \frac{\alpha_1 \alpha_2 A_s}{b}\right) f_{cd};\ q_3 = M - \alpha_1 f_{cd} d A_s + \frac{\alpha_1^2 f_{cd}}{2b} A_s^2 \tag{5}$$

$$q_1 A_{st}^2 + q_2 A_{st} + q_3 = 0 \tag{6}$$

$$A_{st} = \frac{-q_2 \pm \sqrt{q_2^2 - 4q_1 q_3}}{2q_1} \tag{7}$$

Only the positive root satisfying physical equilibrium and compatibility was adopted.

To ensure ductile behavior, the strip area determined from Eq. (7) should be verified against the EC2 ductility requirement, which limits the neutral axis depth to $x/d \leq 0.45$ for concrete classes up to C50. Strip areas yielding neutral axis depths exceeding this limit should be reduced accordingly.

Table 8 presents a comparison between the moment capacities predicted by Eq. (4), and the experimentally obtained values for all tested specimens. The predicted capacities show good agreement with the experimental results, with an average prediction ratio of 0.82 and a coefficient of variation (CoV) of 9.4%, indicating consistent model performance. As a further check, the flexural capacities were also computed using the ACI 440.2R-17 framework with the Whitney rectangular stress block and nominal measured material properties (American Concrete Institute, 2017). As shown in Table 8, the ACI-based predictions yielded an average Mcal/Mexp ratio of 0.845 with a coefficient of variation of 6.7%, closely consistent with the EC2-based Eq. (4) predictions (average 0.82, CoV 9.4%). The agreement between two independent code-based frameworks provides a useful internal cross-check of the proposed design equation, although full validation against independent experimental datasets remains a subject for future work. Both models are conservative because all strengthened specimens failed in shear before reaching their full theoretical flexural capacity. Although ACI 440.2R-17 is primarily a design guide for FRP strengthening systems, its flexural capacity predictions are grounded in the same Whitney rectangular stress block and sectional equilibrium principles as EC2. Its application here is therefore as an independent sectional analysis framework rather than as an FRP-specific design tool, providing a meaningful basis for cross-checking the EC2-based predictions.

Comparison of calculated and experimental flexural capacities

Specimen	Experimental moment capacity Mexp (kNm)	Eq. (4) Moment capacity Mcal (kNm)	Eq. (4) Mcal/Mexp	ACI Mcal (kNm)	ACI Mcal/Mexp
B0	27.000	20.928	0.775	22.473	0.832
B-Pld	35.250	32.158	0.912	32.395	0.919
B-Str	41.400	32.158	0.777	32.395	0.782
Average			0.821		0.845
Coefficient of variation			0.096		0.067

VI. PRACTICAL IMPLEMENTATION CONSIDERATIONS

NSM mild steel strips offer straightforward constructability. The grooving, bonding, and cover replacement operations require only standard construction tools and commercially available structural epoxy, with no specialist equipment or highly skilled labour. This makes the technique particularly accessible in developing regions where FRP systems may be difficult to source or apply.

Corrosion is a legitimate concern for mild steel in structural applications. However, full encasement within concrete and epoxy provides adequate protection under normal exposure conditions. In aggressive environments — marine or highly humid conditions, for instance — additional corrosion protection such as epoxy coating of the strips prior to installation is advisable. Periodic inspection of the concrete cover for cracking or delamination is recommended as a routine maintenance measure to ensure long-term performance.

VII. LIMITATIONS OF THE STUDY

The findings of this study are based on static monotonic loading. The behaviour of NSM mild steel strip strengthening under fatigue, cyclic loading, and long-term durability conditions was not investigated.

The preloading level adopted in this study represents the onset of in-service damage. The behaviour of NSM mild steel strip strengthening applied to severely damaged structures was not investigated.

Crack width measurements were not taken during testing. Future investigations incorporating quantitative crack monitoring would provide a more complete characterisation of the serviceability behaviour of NSM mild steel strip strengthened beams.

VIII. CONCLUSION

The paper experimentally investigated the effect of near-surface-mounted steel strips on flexural performance of normal reinforced concrete beams. The following conclusions were drawn from the observed results discussed above:

i. Failure modes followed diagonal tension shear failure in both the initially weakened (preloaded) and directly strengthened flexure dominant specimens, as compared to the control beam that failed in flexure. Introduction of hot rolled mild steel strips therefore changed the collapse modes in the beam elements.
ii. Generally, first crack was observed at higher loads in the strengthened specimens compared to the controls, i.e., at 99% and 129% above the control cracking load, for preloaded and directly strengthened beams respectively. Mild steel strips therefore delayed initiation of crack.
iii. Ultimate loads increased by 30% and 53% in the preloaded and directly strengthened beams

respectively. Thus, mild steel strips enhance flexural capacity in normal concrete beams.

iv. Energy absorption was governed primarily by the failure mode of the beams. The control beam exhibited greater energy absorption due to its ductile flexural behavior and significant post-peak deformation. Strengthened beams absorbed less energy because failure shifted to brittle shear. Thus, higher strength did not necessarily correspond to higher energy absorption.

v. Elastic stiffness generally increased following strengthening, indicating improved resistance to initial deformation. Stiffness enhancement was moderate, with preloading slightly limiting improvement. Overall, strengthening effectively enhanced the elastic response of the beams.

Bond behaviour between the NSM mild steel strips, epoxy adhesive, and surrounding concrete was not debonding-critical in this study, as no debonding indicators were observed throughout testing. A detailed investigation of this aspect is recommended as a subject of future study.

AUTHOR CONTRIBUTIONS

N. J. Ateny: Conceptualization of the study, development of methodology, experimental investigation, data curation and formal analysis, visualization of results, and preparation of the original manuscript draft. **David O. Koteng**: Supervision, methodological guidance, validation of experimental procedures and results, critical review of the manuscript, and editing of the final version. **S. M. Shitote**: Academic supervision, project administration, validation of research outcomes, provision of scholarly guidance, and critical review and editing of the manuscript.

ACKNOWLEDGMENTS

We are grateful to the African Union for their scholarship grant which made working on this research a reality. Most of the civil engineering academic staff of the Pan African University Institute for Basic Sciences, Technology and Innovation (PAUSTI) have been helpful through meticulous guidance, supervision and review, and we appreciate their inputs.

FUNDING

The work was funded by the African Union scholarship.

CONFLICTS OF INTEREST

The authors declare that there is no conflict of interest regarding this article.

REFERENCES

Altin, S., Kopraman, Y., and **Baran, M.** (2013). Strengthening of RC walls using externally bonding of steel strips. Engineering Structures, 49, 686–695. https://doi.org/10.1016/j.engstruct.2012.12.022

American Concrete Institute. (2017). ACI 440-2R-17: Guide for design and construction of FRP systems for strengthening of concrete structures.

Askar, M. K., Hassan, A. F., and **Al-Kamaki, Y. S. S.** (2022). Flexural and shear strengthening of reinforced concrete beams using FRP composites: A state of the art. Case Studies in Construction Materials, 17, Article e01189. https://doi.org/10.1016/j.cscm.2022.e01189

Awad, F., Husain, M., and **Fawzy, K.** (2022). Flexural behavior of reinforced concrete beams strengthened with NSM ECC. Frattura ed Integrità Strutturale, 16(60), 291–309. **https://doi.org/10.3221/IGF-ESIS.60.21**

Aykaç, S., Kalkan, İ., Aykaç, B., Karahan, S., and **Kayar, S.** (2012). Strengthening and repair of reinforced concrete beams using external steel plates. Journal of Structural Engineering, 139(6), 929–939. **https://doi.org/10.1061/(ASCE)ST.1943-541X.0000714**

British Standards Institution, and **European Committee for Standardization.** (2002). BS EN 12390-1-6:2002 Testing hardened concrete.

European Committee for Standardisation, and **International Organisation for Standardization.** (2019). EN ISO 6892-2:2019: Metallic materials – Tensile testing.

European Committee for Standardization. (1998). EN 1097-2:1998: Tests for mechanical and physical properties of aggregates.

European Committee for Standardization. (2000). EN 197-1:2000: Cement – Part 1: Composition, specifications and conformity criteria for common cements.

European Committee for Standardization. (2002). EN 12620:2002: Aggregates for concrete.

European Committee for Standardization. (2004). EN 1992-1-1:2004: Design of concrete structures – Part 1-1: General rules and rules for buildings.

Farooq, S., Islam, Z. U., Jadoon, A. K., Khan, S., and **Khan, M. I.** (2026). Comparison of flexure behavior of beams reinforced with glass fiber reinforced polymers (GFRP) and steel bars. Discover Civil Engineering, 1–28. **https://doi.org/10.1007/s44290-026-00442-w**

Farooq, S. H., Shahid, I., and **Ilyas, M.** (2014). Seismic performance of masonry strengthened with steel strips. KSCE Journal of Civil Engineering, 18(7), 2170–2180. **https://doi.org/10.1007/s12205-014-0540-0**

Hamoda, A., Abadel, A. A., Sennah, K., Ahmed, M., Zhang, X., and **Emara, M.** (2024). Shear strengthening of RC beams incorporating post-tensioned bars and engineered cementitious composite reinforced with palm fronds. Buildings, 14(10), Article 3277. **https://doi.org/10.3390/buildings14103277**

Hamoda, A., Emara, M., Abdelazeem, F., and **Ahmed, M.** (2022). Experimental and numerical analysis of RC beams strengthened with ECC and stainless-steel strips. Magazine of Concrete Research, 75(5), 251–270. **https://doi.org/10.1680/jmacr.22.00127**

Hanu, C., and **Subha, K.** (2018). A review on strengthening techniques using NSM and EBR FRP composites. International Research Journal of Engineering and Technology, 5(4), 3441–3442. **https://www.irjet.net/archives/V5/i4/IRJET-V5I4774.pdf**

Hashemi, S. (2011). Strengthening of concrete structures using carbon fibre reinforced polymers and cement-based adhesives [Doctoral dissertation, Monash University]. **https://doi.org/10.4225/03/589811F857C91**

Haukaas, T. (2026). Euler–Bernoulli beams. University of British Columbia. **https://civil-terje.sites.olt.ubc.ca/files/2026/02/Euler–Bernoulli-Beams.pdf**

Hosen, M. A., Shammas, M. I., Al Kaaf, K. A., Jumaat, M. Z., Alengaram, U. J., Sulong, N. H. R., and **Hashim, H. B.** (2024). Carbon fiber reinforced polymer (CFRP) for structural capacity enhancement of RC beams incorporating innovative side hybrid (SH) technique. Buildings, 14(7), Article 1919. **https://doi.org/10.3390/buildings14071919**

Jing, D. H., Krevaikas, T., and **Zhang, H.** (2021). Prestressed steel strips for the strengthening of axially loaded masonry walls. Structures, 30, 25–40. **https://doi.org/10.1016/j.istruc.2021.01.001**

Kenyan Bureau of Standards. (2018). KS EAS 18-1: 2017: Cement Part 1: Composition, specification and conformity criteria for common cements. **http://www.puntofocal.gov.ar/notific_otros_miembros/ken630_t.pdf**

Marsh, B. K. (1997). Design of normal concrete mixes (2nd ed.). Construction Research Communications.

Moghaddam, H., Samadi, M., Pilakoutas, K., and **Mohebbi, S.** (2010). Axial compressive behavior of concrete actively confined by metal strips; Part A: Experimental study. Materials and Structures, 43(10), 1369–1381. **https://doi.org/10.1617/s11527-010-9588-6**

Oller, E., Pujol, M., and **Marí, A.** (2019). Contribution of externally bonded FRP shear reinforcement to the shear strength of RC beams. Composites Part B: Engineering, 164, 235–248. **https://doi.org/10.1016/j.compositesb.2018.11.065**

Rasheed, H. A., **Harrison, R. R.**, **Peterman, R. J.**, and **Alkhrdaji, T.** (2010). Ductile strengthening using externally bonded and near surface mounted composite systems. Composite Structures, 92(10), 2379–2390. **https://doi.org/10.1016/j.compstruct.2010.03.009**

Raza, S., Khan, M. K. I., Menegon, S. J., Tsang, H. H., and **Wilson, J. L.** (2019). Strengthening and repair of reinforced concrete columns by jacketing: State-of-the-art review. Sustainability, 11(11), Article 3208. **https://doi.org/10.3390/su11113208**

Rizzo, A., and **De Lorenzis, L.** (2009). Behavior and capacity of RC beams strengthened in shear with NSM FRP reinforcement. Construction and Building Materials, 23(4), 1555–1567. **https://doi.org/10.1016/j.conbuildmat.2007.08.014**

Sabau, C., Popescu, C., Sas, G., Schmidt, J. W., Blanksvärd, T., and **Täljsten, B.** (2018). Strengthening of RC beams using bottom and side NSM reinforcement. Composites Part B: Engineering, 149, 82–91. **https://doi.org/10.1016/j.compositesb.2018.05.011**

Tarabia, A. M., and **Albakry, H. F.** (2014). Strengthening of RC columns by steel angles and strips. Alexandria Engineering Journal, 53(3), 615–626. **https://doi.org/10.1016/j.aej.2014.04.005**

Yang, Y., Chen, X., Xue, Y., and **Yu, Y.** (2022). Experimental investigation on shear performance of reinforced concrete beams retrofitted by pre-stressed steel strips. Structures, 43, 767–778. **https://doi.org/10.1016/j.istruc.2022.07.013**

Zhang, S. S., Yu, T., and **Chen, G. M.** (2017). Reinforced concrete beams strengthened in flexure with near-surface-mounted (NSM) CFRP strips: Current status and research needs. Composites Part B: Engineering, 131, 30–42. **https://doi.org/10.1016/j.compositesb.2017.07.072**